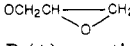
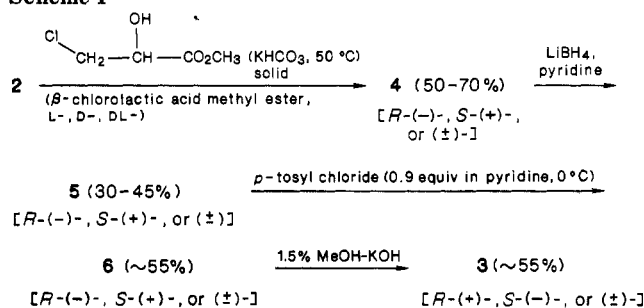




**Table I.** Physicochemical Properties of Carbon-7-Substituted Model Analogues of Actinomycin D

compd	R	ep, <sup>a</sup> %	mol formula	t <sub>R</sub> , <sup>b</sup> min	[α] <sub>D</sub> <sup>20</sup> , deg (c, CHCl <sub>3</sub> ) <sup>c</sup>	<sup>1</sup> H NMR signal for R, δ <sup>b</sup> (δ values in brackets are for CH(OH) proton only)
1a	H		C <sub>20</sub> H <sub>22</sub> N <sub>4</sub> O <sub>4</sub>	11.8	±0	7.33 (s, 1 H)
2a	OH		C <sub>20</sub> H <sub>22</sub> N <sub>4</sub> O <sub>5</sub>	15.6	±0	6.80 (s, 1 H)
3a		0	C <sub>23</sub> H <sub>26</sub> N <sub>4</sub> O <sub>6</sub>	23.5, 21.1	±0	3.7 (d, 2 H), 4.12 (m, 1 H)
	R-(+) enantiomer	90		23.5	+8.8 (5.1)	[3.98 (m, 1 H)]
	S-(-) enantiomer	90		20.9	-8.8 (5.0)	[4.20 (m, 1 H)]
4a	OCH <sub>2</sub> CH(OH)COOCH <sub>3</sub>	0	C <sub>24</sub> H <sub>28</sub> N <sub>4</sub> O <sub>8</sub>	34.0, 36.8	±0	2.85 (s, 3 H, CH <sub>3</sub> ), 4.56 (t, 1 H), 3.36 (d, 2 H), 6.90 (d, 1 H), (peak at 6.90, D <sub>2</sub> O exchangeable)
	R-(-) enantiomer	97		34.0	-4.8 (11.0)	[4.44 (t, 1 H)]
	S-(+) enantiomer	97		37.0	+4.7 (11.3)	[4.68 (t, 1 H)]
5a	OCH <sub>2</sub> CH(OH)CH <sub>2</sub> OH	0	C <sub>23</sub> H <sub>28</sub> N <sub>4</sub> O <sub>7</sub>	30.1, 28.0	±0	3.75 (d, 2 H), 4.2-4.35 (1 H), 3.20 (d, 2 H), 6.92 (br, 1 H), 7.1 (br, 1 H)
	R-(-) enantiomer	95		30.9	-6.8 (7.7)	[4.24 (dd, 1 H)]
	S-(+) enantiomer	95		28.5	+6.1 (7.5)	[4.33 (dd, 1 H)]
6a	OCH <sub>2</sub> CH(OH)CH <sub>2</sub> OTS	0	C <sub>30</sub> H <sub>34</sub> N <sub>4</sub> O <sub>9</sub> S	20.8, 22.7	±0	2.42 (s, 3 H), 4.15 (dd, 4 H), 6.88 (1 H), 4.95 (m, 1 H), 7.43 (2 H), 7.7 (d, 2 H)
	R-(-) enantiomer	90		20.5	-7.8 (4.6)	[4.90 (m, 1 H)]
	S-(+) enantiomer	90		22.7	+7.5 (4.4)	[4.99 (m, 1 H)]
7a	OCH <sub>2</sub> CH(OR-(+)-MTPA)CH <sub>2</sub> OR-(+)-MTPA		C <sub>43</sub> H <sub>42</sub> N <sub>4</sub> O <sub>11</sub> F <sub>6</sub>	6.6, 9.9	±0	5.18 (q, 3 F), 4.91 (q, 3 F), <sup>e</sup> 4.70-4.00 (overlapping, 6 F)
	R-(+), R-(-) enantiomer	95		6.1	-54.0 (1.0)	5.22 (q, 3 F), 4.74 (q, 3 F)
	R-(+), S-(+) enantiomer	95		9.8	+50.9 (1.2)	4.90 (q, 3 F), 4.09 (q, 3 F)

<sup>a-e</sup> Please refer to Table II for explanation of these notations.**Scheme I**

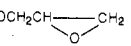
lution on a chiral HPLC column or by asymmetric epoxidation of an intermediate olefin were unsuccessful (vide supra). The synthesis of the enantiomers of analogues 3-7 in relatively pure forms (>90%) (Chart I) was carried out following the sequence of reactions shown in Scheme I. DL-, D-, or L-halo lactic acid methyl esters were condensed with 7-hydroxy analogues 2 (a or b) by using solid potassium bicarbonate in a heterogeneous-phase reaction according to our previously reported procedure, yielding the enantiomers of 7-(2-hydroxy-2-carbomethoxyethoxy) chain substituted compounds (4) in 97% purity and in good to moderate yields, depending on the starting (2a or 2b) compound and the halo ester employed (see the Experimental Section). These products were converted to the 7-(2,3-dihydroxypropoxy) chain substituted analogues (5) by a LiBH<sub>4</sub> in pyridine mediated reduction of the carbomethoxy group. The enantiomeric forms of 5 were obtained in >95% purity and in 30-45% yield. The resulting dihydroxy chain substituted compounds were selectively tosylated to 7-(2-hydroxy-3-tosyloxy) chain substituted analogues (6) by reacting with a subequimolar [(0.9 molar ratio of *p*-toluenesulfonyl (*p*-tosyl) chloride] at 0 °C in order to tosylate only the primary 3-hydroxyl function and to prevent reaction on the secondary 2-hydroxyl function, which might lead to decreased enantiomeric purity of the products. The progress of the reaction was monitored by HPLC and NMR, and the products were

identified by their physicochemical characteristics, including elemental and mass spectrometric analysis. The tosyl derivatives in enantiomeric purity of >90% were isolated in moderate yields, and these were cyclized to oxirane (epoxy) rings by the trans side elimination of the monotosyl function by reaction with 1.5% methanolic KOH at ambient temperature. Thus the R-(-) enantiomer of 6 produced the R-(+) enantiomer of 3. The reaction was monitored by TLC for actinomycin analogue (6b), insuring that no rupture of the peptide lactone rings occurred during the course of this reaction in methanolic KOH.<sup>5</sup> The final products in enantiomeric forms were isolated in yields of about 55% without any appreciable racemization and in enantiomeric excess of 80% (90% purity). As mentioned earlier, the sequence of reactions was carried out initially on the model analogues from which the optimal reaction conditions were established. The enantiomeric purity and characterization of the enantiomers in the actinomycin series were established primarily by HPLC and corroborated by NMR, whereas in the model series (series a) the characterization was first made on the basis of the optical rotatory and NMR behaviors, and the purity was estimated by NMR and HPLC. (The physicochemical data for analogues are in Tables I and II.)

The enantiomeric purity of the crucial dihydroxy-chain analogues (5a and 5b) and the final oxirane-ring products 3a and 3b was further verified by the following techniques. The 7-(2,3-dihydroxypropoxy)actinomycin and the model analogues were converted to their di-(R)-(+)-MPTA acid ester derivatives (7) by reaction of (R)-(+)-α-methoxy-α-(trifluoromethyl)phenylacetyl chloride [(R)-(+)-MPTA chloride, Chart I], and the <sup>19</sup>F NMR of these derivatives<sup>6</sup> were examined (Tables I and II). The second method made use of a chiral shift agent Eu(hfc)<sub>3</sub> [[3-(hepta-

(5) Tattersall, M. H. N.; Sodergren, J. E.; Sengupta, S. K.; Trites, D. H.; Modest, E. J.; Frei, E., III. *Clin. Pharm. Ther.* 1975, 17, 701.(6) Dale, J. A.; Dull, D. A.; Mosher, H. A. *J. Org. Chem.* 1969, 34, 2543.

**Table II.** Physicochemical Properties Carbon-7-Substituted Analogues of Actinomycin

compd	R	ep, <sup>a</sup> %	mol formula	t <sub>R</sub> , <sup>b</sup> min	[α] <sub>D</sub> <sup>20</sup> , deg (c, CHCl <sub>3</sub> ) <sup>c</sup>	<sup>1</sup> H NMR signal for 2-CHOH (R) proton only, δ <sup>d</sup>
1b	H		C <sub>82</sub> H <sub>86</sub> N <sub>12</sub> O <sub>16</sub> ·2H <sub>2</sub> O	16.9	-360 ± 22 (0.15)	7.53
2b	OH		C <sub>82</sub> H <sub>88</sub> N <sub>12</sub> O <sub>17</sub> ·H <sub>2</sub> O	19.0	-298 ± 20 (0.15)	8.11
3b		0	C <sub>86</sub> H <sub>90</sub> N <sub>12</sub> O <sub>18</sub> ·2H <sub>2</sub> O	30.0, 26.7	-400 ± 25 (0.15)	3.98-4.11 (m, 1 H)
	<i>R</i> -(+) enantiomer	90		30.1	-380 ± 20 (0.15)	3.99 (m, 1 H)
	<i>S</i> -(-) enantiomer	90		26.5	-408 ± 18 (0.15)	4.21 (m, 1 H)
4b	OCH <sub>2</sub> CH(OH)COOCH <sub>3</sub>	0	C <sub>66</sub> H <sub>92</sub> N <sub>12</sub> O <sub>20</sub> ·2H <sub>2</sub> O	46.7, 43.3	-201 ± 15 (0.15)	4.55-4.88 (t, 1 H)
	<i>R</i> -(-) enantiomer	97		46.7	-207 ± 15 (0.15)	4.50 (t, 1 H)
	<i>S</i> -(+) enantiomer	97		43.0	-200 ± 15 (0.15)	4.77 (t, 1 H)
5b	OCH <sub>2</sub> CH(OH)CH <sub>2</sub> OH	0	C <sub>65</sub> H <sub>92</sub> N <sub>12</sub> O <sub>19</sub> ·2H <sub>2</sub> O	40.5, 36.7	-308 ± 15 (0.15)	4.33-4.50 (m, 1 H)
	<i>R</i> -(-) enantiomer	95		40.0	-322 ± 12 (0.12)	4.35 (m, 1 H)
	<i>S</i> -(+) enantiomer	95		36.0	-299 ± 15 (0.15)	4.45 (m, 1 H)
6b	OCH <sub>2</sub> CH(OH)CH <sub>2</sub> OTS	0	C <sub>72</sub> H <sub>88</sub> N <sub>12</sub> O <sub>21</sub> S	27.8, 21.8	-101 ± 12 (0.20)	4.97-5.11 (m, 1 H)
	<i>R</i> -(-) enantiomer	90		28.0	-103 ± 10 (0.30)	4.90 (m, 1 H)
	<i>S</i> -(+) enantiomer	90		21.2	-98 ± 11 (0.30)	5.10 (m, 1 H)
7b	OCH <sub>2</sub> CH(OR-(+)-MTPA)CH <sub>2</sub> OR-(+)-MTPA	0	C <sub>85</sub> H <sub>106</sub> N <sub>12</sub> O <sub>23</sub> F <sub>6</sub> ·H <sub>2</sub> O	7.7, 5.7	-253 ± 30 (0.30)	5.22-4.48 (m, 12 F) <sup>e</sup>
	<i>R</i> -(+), <i>R</i> -(-) enantiomer	95		8.0	-230 ± 30 (0.30)	5.28 (q, 3 F), 4.80 (q, 3 F)
	<i>R</i> -(+), <i>S</i> -(+) enantiomer	95		5.0	-238 ± 30 (0.30)	4.97 (q, 3 F), 4.45 (q, 3 F)

<sup>a</sup> Enantiomeric purity (percent) indicates percent population of the major enantiomer. <sup>b</sup> Retention time in HPLC in minutes, with a Varian MCH-10 C<sub>18</sub> column and a pH 7 Tris-phosphate buffer solution containing 2.5% methanol as an eluant. <sup>c</sup> Concentration denoted by c in grams/100 milliliters. <sup>d</sup> Proton NMR spectra were obtained on a JEOL FQ 90-90MHz or 300-MHz Varian XL spectrometer with deuteriochloroform as solvent and approximately 2% tetramethyl silane as an internal standard. <sup>e</sup> The fluorine NMR spectra were determined with a Varian HA-100 (94.1 MHz) spectrometer with a solvent mixture of 80% of deuteriochloroform and approximately 20% trifluoroacetic acid by volume as an internal standard added immediately prior to the determination; alternatively, it was used as an external standard when the investigations were to be carried for a prolonged period to avoid any destructive reaction of this acid on samples.

fluoropropyl)hydroxymethylene]-*d*-camphorato]europium(III)].<sup>7</sup> This reagent shifted the NMR peaks of the methine (CHO) proton in the oxirane ring downfield and resolved the complex multiplets observed in the spectra of the racemic **3a** and **3b** into two simple sets of multiplets centered at δ 5.29 for the *R*-(+) enantiomer and at δ 5.49 for the *S*-(-) enantiomer, respectively. The integration in the NMR peaks gives the amount of the enantiomeric purity (%) of the isomers.

As observed earlier, attempts were made to resolve the racemic mixtures of (±)-EPA by chromatography on chiral HPLC columns. With use of a Pirkle I-A column packed with (*R*)-*N*-[(3,5-dinitrobenzoyl)phenyl]glycine ionically bonded to aminopropyl siliconized silica (Experimental Section) and with use of 20% MeOH-20 mM NH<sub>4</sub>OAc, pH 6.6 as eluant, we could enrich the components to about 66:33 (2:1) ratios. The enriched *R*-(+) component, tested in vitro against CCRF-CEM and L1210 leukemia cell lines, demonstrated superior activities compared to either the racemic and *S*-(-)-enriched mixtures. Estimation of the enantiomeric percentage in each mixture was made by the resolution of the methine peaks with NMR chiral shift agent Eu(hfc)<sub>3</sub>, and integration of the peak areas. All attempts to resolve these mixtures any further failed, probably because of the formation of formidable eutectics that are not resolvable by simple HPLC procedures. Next, a single-step asymmetric epoxidation to the desired enantiomers was attempted via the procedure reported recently by Groves and Meyers.<sup>7</sup> With 7-(allyloxy)actinomycin D<sup>8</sup> as the starting material, oxirane ring formation was attempted with the use of a chiral catalyst FeT(α,β,α,β-Binap)PPCl and iodosylmesitylene as an oxidant. In this procedure, the asymmetry is reported to be induced selectively by a transfer of an oxygen atom from the iodosyl group through the intermediacy of the oxidized iron-porphyrin catalyst. The stereochemistry of the epoxy product is presumed to be conferred by the conformational

mobility of the chiral appendages and the nonbonded interaction between the catalyst and the substrate surfaces. The procedure is complex, and the isolation of products requires extensive purification with TLC, which again yielded another mixture of components; however, the *R*-(+) isomer was obtained in an enantiomeric ratio of 7:3 in good yield (69%), and this mixture showed further promising activity in in vitro HT-29 human colon carcinoma and in vivo L1210 leukemia. Thus, even these partially enriched enantiomeric forms provided us with important information about the *R*-(+) enantiomer as the primary active component of (±)-EPA.<sup>9</sup>

The biochemical and the biological studies reported in this paper were done by using the aforementioned 90% enantiomeric purity (90:10) of (*R*)-(+)-EPA and (*S*)-(-)-EPA; the properties and the activities of the enantiomers

(7) Groves, J. T.; Myers, R. S. *J. Am. Chem. Soc.* **1983**, *105*, 5791.

(8) Sehgal, R. K.; Almassian, B.; Rosenbaum, D. P.; Zadrozny, R.; Sengupta, S. K. *J. Med. Chem.* **1987**, *30*, 1626.

(9) Note: A reviewer has commented that a probable alternative method of epoxidation could be the one reported by Sharpless and co-workers, which was devised primarily for enantioselective epoxidation of stereoisomeric allylic alcohols (*J. Am. Chem. Soc.* **1980**, *102*, 5974; **1981**, *103*, 464). This procedure is highly stereoselective when the pure single stereoisomeric form of only allylic alcohol is used. More recently, the synthesis of pure stereoisomeric styrene oxides has been reported by an analogous procedure, apparently with a similarly pure isomer of certain styrene analogues as starting material, by Imanari Makato and his group, in a Japanese patent (*Chem. Abstr.* **1986**, *104*, 224829f). The prerequisite for both is stereochemical purity of the starting olefin.

(10) Sengupta, S. K.; Kogan, Y.; Kelley, C.; Szabo, J. *J. Med. Chem.* **1988**, *31*, 768.

(11) Farber, S. *JAMA, J. Am. Med. Assoc.* **1966**, *198*, 826.

(12) Vogel, C. K.; Primack, A.; Dhru, D.; Briers, P.; Owor, R.; Ky-alwazi, S. K. *Cancer* **1973**, *31*, 1382.

(13) Cragoe, E. J.; Robb, C. M. *Org. Synth.* **1960**, *40*, 54.

(14) Hirschbein, B. L.; Whitesides, G. M. *J. Am. Chem. Soc.* **1982**, *104*, 4458.

(15) Matos, J. R.; Smith, M. B.; Wong, C.-H. *Bioorg. Chem.* **1985**, *13*, 121.

(16) Dale, J. A.; Mosher, H. S. *J. Org. Chem.* **1970**, *35*, 4002.

(17) Pollak, A.; Blumenfeld, H.; Wax, M.; Baughn, R. L.; Whitesides, G. M. *J. Am. Chem. Soc.* **1980**, *102*, 6324.

(18) Inaba, M.; Johnson, R. K. *Cancer res.* **1977**, *37*, 4629.

**Table III.** Covalent and Noncovalent (Intercalative) Binding to Calf Thymus DNA. Antitumor Activity (in Vitro and in Vivo) against Actinomycin Resistant (P388/ADR) and in Vitro Activity in Sensitive (B16) Cells by Actinomycin Analogues

compd	$\Delta T_m^a$	[DNA base]/[drug]		inhibition of growth ID <sub>50</sub> , <sup>d</sup> nM		antitumor activity against P388/ADR, in ip implanted CDF <sub>1</sub> mice, treated ip, qd 1-9		
		A <sup>b</sup>	B <sup>c</sup>	P388/ADR	B16	OD <sup>e</sup>	MST, <sup>f</sup> days	% ILS (surv) <sup>g</sup>
1b (AMD)	7.1 ± 0.15	26 ± 2	ND	2500 ± 250	3.0 ± 1.0	0.075	12	33 (0/10)
3b [(±)-EPA]	5.2 ± 0.95	32 ± 1	480 ± 10	80 ± 11	2.5 ± 0.6	0.65	40	344 (4/10)
(R)-(+)-EPA	4.8 ± 1.15	30 ± 2	500 ± 15	40 ± 12	2.0 ± 0.4	0.30	45	400 (4/10)
(S)-(-)-EPA	5.0 ± 1.10	32 ± 2	520 ± 15	135 ± 12	3.5 ± 1.0	0.80	43	377 (5/10)
mitomycin c						1.0	45	400 (5/10)

<sup>a</sup>  $\Delta T_m = T_m$  of DNA-drug complex minus  $T_m$  of drug-free DNA; concentration of drug 14.0 nM and that of DNA 70 nM in 0.01 M phosphate buffer, pH 7.0, 5 × 10<sup>3</sup> EDTA and 5% Me<sub>2</sub>SO. Broad  $\Delta T_m$  of analogues indicate some covalent binding, in contrast to relatively sharp  $T_m$  of actinomycin that is indicative of intercalative binding to DNA. <sup>b</sup> Binding to purified calf thymus DNA in 20 mM Tris-HCl, pH 7.4 buffer at 37 °C; A values are molar ratios of DNA to drug based on the total amount of drug that is bound both intercalatively and covalently to DNA helix. <sup>c</sup> B values are similar ratios assayed on the basis of drugs bound entirely by covalent bonding to DNA base. <sup>d</sup> Concentration required for 50% inhibition of growth of actively growing tumor cells in vitro. <sup>e</sup> Optimal dose of drugs. <sup>f</sup> Median survival time of tumor bearing mice. <sup>g</sup> Percent increase in median life time in days of drug-treated and dying animals vs those of controls; (survivors), number of >60 days survivors/number of animals tested in the group.

**Table IV.** pH-Dependent Ultraviolet Absorption of Synthetic (HPLC Identified) Deoxyguanosine-EPA Adducts

site specific adducts (HPLC peak product)	$\lambda_{max}$ , nm		
	acid (0.1 N HCl)	neutral <sup>a</sup> (pH 6.9)	alkaline (0.1 N NaOH)
N <sup>7</sup> -dG			
(EPA IV-dG)	257 <sup>b</sup> (256, 280, sh <sup>d</sup> ) <sup>e</sup>	263, 285 (263, 285)	266 <sup>c</sup> (266)
O <sup>6</sup> -dG			
(EPA II-dG)	247, 287	247, 282	250, 282
(EPA III-dG)	243, 288 (243, 288) <sup>e</sup>	252, 282 (247, 282) <sup>e</sup>	247, 282 (248, 281) <sup>e</sup>
N <sup>2</sup> -dG			
(EPA I-dG)	263 (259)	253 (253)	257 (257, 270 sh)

<sup>a</sup> The spectra were recorded with equimolar (R)-(-) and (S)-(+)-DHPA solutions in the blank cuvette; 0.1 M PO<sub>4</sub><sup>3+</sup> buffer. <sup>b</sup> Spectra recorded within 5 min after preparation of the acid solution at a low temperature (0 °C); at ≥80 °C in 30 min deglycosylation takes place, which is consistent with N<sup>7</sup>-dG substitution (mass spectra data). <sup>c</sup> Possibly of the anion of the imidazole ring opened ring (see reference below). <sup>d</sup> Sh, shoulder. <sup>e</sup> Data in the parentheses: reported data of the corresponding benzyl analogue substituted dG-adducts.<sup>21</sup>

are reported in Tables II-V.

**DNA-Binding Studies. Thermal Denaturation of DNA-Drug Complexes.** These experiments were carried out according to our previously reported procedures.<sup>1</sup> As before, the thermal denaturation studies of calf thymus DNA complexed with synthetically pure (90%, Table II) optical isomeric forms (R)-(+)-EPA and (S)-(-)-EPA establish what was already observed for the racemic (±)-EPA; i.e., in contrast to actinomycin D ( $\Delta T_m$ , 7.1 ± 0.15), these enantiomers produced broad  $\Delta T_m$  values (~5.0 ± 1.15, Table III) like the racemic form (±)-EPA [(±)-3b], indicating their DNA alkylating activity; however, positive (e.g. ≈ +5.0 °C) elevations of the melting temperatures by the DNA-drug complex also indicated that the drugs might be binding simultaneously via interaction.<sup>8</sup> Recently, by using agarose gel electrophoresis of a closed circular duplex DNA complexed with drugs, we have confirmed that these agents do bind to DNA intercalatively.<sup>8</sup>

**Relaxation of Supercoiled Closed-Circular DNA.** Via a procedure similar to that of Keller,<sup>19</sup> we attempted to qualitatively compare the unwinding produced by actinomycin D analogues with that produced by ethidium bromide (EBR). This involved closed-circular DNA that

is nicked and ligated with DNA-relaxing enzyme in the presence of the drug, followed by agarose gel electrophoresis. The experiments gave uniform results, demonstrating that like AMD and EBR, the enantiomers (R)-(+)-, (S)-(-)-, and (±)-EPA relax the supercoiling of the closed-circular SV40 DNA in a progressive dose-dependent manner, providing direct evidence that the analogues intercalate into DNA (Figure 1, supplementary material).

**Determination of the Ratios of DNA Base to Drug during Intercalative (B) and Covalent (A) Drug Bindings.** These ratios were estimated according to procedures reported by us previously.<sup>2</sup> In brief, [<sup>3</sup>H]drug and calf thymus DNA in 25 mM Tris-HCl buffer was dialyzed at 37 °C, and the equilibrated complex was precipitated twice with ethanol, which freed it completely from the unbound drug. This DNA-drug complex contained bound [<sup>3</sup>H]drug, associated both intercalatively and covalently; the ratio of the DNA base to bound drug was estimated by the absorbance for the bases at 260 nM (after correction for the contribution from the drug molecule) and by the specific activity for the drug; the number of DNA bases per bound drug molecule gives A.<sup>2</sup> The intercalatively bound drug was then removed by denaturation of DNA by sequential dialysis in the presence of high salt and urea followed by precipitation with EtOH. Estimation of the number of DNA bases per drug molecule (B) gives an extent of covalent binding. The values of A and B (Table III) for the enantiomers are nearly the same, indicating that the intercalative and covalent bond forming abilities of these three optical isomeric forms of EPA are practically identical. However, the enantiomers clearly demonstrate a difference in the preference for the sites of alkylation in guanine bases in DNA.

**Identification of DNA Adducts.** In a previous paper<sup>2</sup> we reported that the (±)-EPA-DNA adducts, after enzymatic digestion and resolution in HPLC, generate three identifiable peaks. Authentic deoxynucleotide adducts, synthesized by reaction of (±)-EPA with deoxynucleotides, helped to identify these peaks in the HPLC as solely deoxyguanosine adducts. These peaks were labeled as EPA II-dG, EPA III-dG, and EPA IV-dG. Another synthetic peak EPA I-dG in the HPLC was not isolated from the enzymatic digest. Of late, we have synthesized all four adducts by reaction between (R)-(+)-EPA and (S)-(-)-EPA and deoxyguanosine, via our reported procedure.<sup>2</sup> The (R)-(+)-isomer produced EPA I-dG and EPA IV-dG and (S)-(-)-EPA generated EPA II-dG and EPA III-dG peaks. In the DNA-adduct digest EPA IV-dG was the major adduct (over 70%) and EPA II-dG and EPA III-dG accounted for the remaining adducts. The (R)-(+)-enantiomer

**Table V.** Inhibition of Nucleic Acid Synthesis, Growth in Vitro and in Vivo of L1210 Murine Leukemia Cells by Actinomycin D and Enantiomers of (±)-EPA

compd	inhibition of synthesis of nucleic acids in L1210: IC <sub>50</sub> , <sup>a</sup> μM		inhibition of growth of L1210 cells in culture: ID <sub>50</sub> , <sup>d</sup> nM	activity in mice bearing leukemia L1210	
	DNA <sup>b</sup>	RNA <sup>c</sup>		OD <sup>e</sup>	% ILS <sup>f</sup> (surv) <sup>g</sup>
1b (AMD)	0.38 ± 0.028	0.019 ± 0.006	60.1 ± 9.8	0.025	55 (0/9)
3b [(±)-EPA]	0.08 ± 0.019	0.024 ± 0.004	28.7 ± 8.7	0.05	186 (2/9)
(R)-(+)-EPA	0.06 ± 0.015	0.031 ± 0.005	23.1 ± 7.7	0.05	199 (3/9)
(S)-(-)-EPA	0.06 ± 0.010	0.050 ± 0.005	56.8 ± 8.8	0.05	143 (1/9)

<sup>a</sup> Drug concentration (micromolar) for 50% reduction of incorporation of [methyl-<sup>14</sup>C]thymidine into DNA (b) and [5-<sup>3</sup>H]uridine into RNA (c) from the rate of incorporation of the same radionucleotides in non-drug-treated L1210 cells growing actively in vitro. <sup>d</sup> Drug concentration (nanomolar) for 50% inhibition of growth relative to growth of non-drug-treated L1210 cells. <sup>e</sup> OD, optical dose of drugs in milligrams/kilogram per injection, administered ip on days 1, 5, and 9, following ip inoculation with 10<sup>5</sup> L1210 cells per CDF<sub>1</sub> mouse on day 0. <sup>f</sup> % ILS, percent increase in median life span in days, of the tumor-bearing drug-treated dying animals when compared with similar tumor bearing mice but not treated with drugs. <sup>g</sup> (surv), number of over 60 days survivors/number of animals tested.

was found to produce over 80% of the EPA IV-dG adduct while the S-(-) enantiomer produced over 70% of the EPA II-dG and EPA III-dG peak material in HPLC, along with some DHPA (~8%), which might have originated from an unknown labile conjugate.<sup>2</sup> Difference absorbance and circular dichroism spectral behaviors (Figure 2 in supplementary material and Table IV) of the peak eluted materials strongly suggest that the EPA IV-dG peak products should be the (R)-(-)-N<sup>7</sup>-deoxyguanosine-substituted adduct and that both EPA II-dG and EPA III-dG peak materials are, most likely, the positional isomers of (S)-(+)-O<sup>6</sup>-deoxyguanosine substituted products (see Figure 3 in supplementary material for proposed structures). The pH-dependent ultraviolet absorption properties of the EPA-dG adducts are tabulated (Table IV); these spectra were taken with the dihydroxy compounds **5a** or **5b** as blanks to accentuate the peak positions. The data demonstrate characteristic absorption peaks for the individual adducts, and these properties agree reasonably well with those reported for alkyl (benzyl) substituted deoxyguanosine derivatives.<sup>21</sup> Among these, the N<sup>7</sup>-substituted adduct (both in the actinomycin **b** and model **a** series) was further characterized by the loss of a pentose group on treatment with acid (0.1 N HCl) at high temperature (70 °C) according to the method of Lawley,<sup>20</sup> giving a sugar-free 7-guanine adduct, which was identified by HPLC and TLC properties. This guanine adduct from the model (R)-(-)-N<sup>7</sup>-conjugate was analyzed further by using negative ion fast atomic bombardment mass spectrometry, *m/z* 589 (M - H). However, a more detailed investigation with high-resolution NMR, using both one- and two-dimensional experiments (COSY and NOESY techniques), is necessary before the exact configuration and conformation of these adducts can be established, and these are presently being investigated.<sup>22</sup>

The above results (Table IV) point to certain distinguishing characteristics that these two enantiomers demonstrate during adduct formation, that is, the R-(+) and S-(-) enantiomers exhibit preferences for separate and defined sites on the deoxyguanosine base in DNA (N<sup>7</sup> vs O<sup>6</sup>), although neither enantiomer exhibits measurable differences in their quantitative interaction with this base in DNA (Table III). This site specific adduct formation might in some way be related to their respective DNA-dependent biological activity. If this property of DNA-base substitution is the major source of their biological activity,

then it might explain, in part, the difference in the biological activity demonstrated by the enantiomers.

**Biological Activity in Vitro. Cell Growth Inhibitory Potency (ID<sub>50</sub>).** The analogues were assayed for in vitro growth inhibitory activity against several experimental tumor lines including human and murine leukemia, mouse melanoma, and human lymphoblastic leukemia. Early investigations employing a moderately pure (>66%) R-(+) isomer against CCRF-CEM cell lines gave the first evidence that the R-(+) isomer of EPA is the major active component. Later, with a purer (>90%) form of R-(+) and S-(-) isomers, the 50% growth inhibitory dose (ID<sub>50</sub>) for the R-(+) isomer was 2.0 nM compared with a value of 3.5 nM for the S-(-) isomer and 12.5 nM for actinomycin D (data not shown in Tables III and V). Against the murine leukemia L1210, which is less responsive to actinomycin, and also against an actinomycin-resistant P388/ADR leukemia via the reported procedure,<sup>18</sup> the R-(+) isomer demonstrates about 3 times the potency of AMD in the L1210 line and more than 60-fold the potency of AMD in the P388/ADR line.<sup>18</sup> The R-(+) isomer is demonstrably superior to actinomycin D in inhibiting the growth of the fast-growing cells; however, this activity in the slower growing B16 mouse melanoma tumor was less pronounced (Tables III and IV).

**Inhibition of Nucleic Acid Synthesis in L1210 Cells in Vitro.** Inhibition of nucleic acid synthesis in L1210 lymphoid leukemia cells by (±)-EPA [(±)-**3b**] and its optical isomers was assayed according to procedures reported with certain modifications.<sup>10</sup> AMD is known to be more effective in inhibiting RNA synthesis than DNA synthesis in cells in culture. Table V shows that in L1210 cells the IC<sub>50</sub> DNA value of AMD is 20 times the IC<sub>50</sub> RNA value, indicating strong preference shown by AMD for blocking RNA synthesis. In contrast, the racemic (±)-EPA, (R)-(+)-EPA, and (S)-(-)-EPA show about 3 to 1, 2 to 1, and 1 to 1 preference, respectively, for the inhibition of RNA to DNA synthesis. Because of the closeness of the IC<sub>50</sub> DNA and IC<sub>50</sub> RNA values for these isomers of EPA (Table V), a modification of the process was introduced in order to account for even a marginal cross-incorporation from the [2-<sup>14</sup>C]uridine into DNA.<sup>10</sup> To achieve this, a digestion of the nucleic acid pellet with DNase-free RNase enzyme, prior to final pelleting of the DNA precipitate, was made to ensure that no more than ±8% contamination from [2-<sup>14</sup>C]uridine into DNA took place, and for this the necessary correction was made in the data reported in Table IV.

These inhibitory data demonstrate that (±)-EPA and its enantiomers are more reactive than AMD in inhibiting replication of DNA, probably by virtue of their dual action on DNA, intercalation as well as alkylation. However, the relative efficiency of cell growth inhibitory activity (L1210,

(20) Lawley, P. D. *IARC Scientific Publ. No 12. International Agency for Research on Cancer*; Lyon, 1976, 181.

(21) Moschel, R. C.; Hudgins, R.; Dipple, A. J. *Org. Chem.* **1984**, *49*, 365.

(22) Sengupta, S. K.; Rosenbaum, D. P. *Proc. Am. Assoc. Cancer Res.* **1987**, *28*, 267.

Table VI. Activity of Actinomycin D Analogues on Mice Inoculated with B16 Melanoma or C26 Colon Carcinoma

compd	B <sub>16</sub> melanoma <sup>a</sup>						C26 colon carcinoma <sup>b</sup>		
	sc-iv			ip-ip					
	OD <sup>c</sup>	MST <sup>d</sup>	%ILS <sup>e</sup> (surv) <sup>f</sup>	OD	MST	%ILS (surv)	OD	MST, days	%ILS (surv)
control		33.0			19.0			22.0	
1b (AMD)	0.9	45.0	36 (0/9)	0.25	29.0	52 (0/9)	0.30	33.5	52 (0/10)
3b [(±)-EPA]	1.0	54.0	64 (0/9)	0.30	39.0	105 (2/9)	0.60	36.0	64 (0/10)
(R)-(+)-EPA	1.0	56.0	70 (1/9)	0.30	39.0	105 (2/9)	0.60	41.5	89 (2/10)
(S)-(-)-EPA	1.0	53.0	60 (1/9)	0.30	33.0	74 (2/9)	0.90	36.0	64 (1/10)
adriamycin	5.0	59.0	79 (1/9)	5.0	60.0	224 (7/9)	2.50	48.0	118 (3/10)

<sup>a</sup> 0.2 mL of brei (tumor weight/Hank's balanced salt solution, 1:5) of B16 implanted sc or ip into groups of nine BDF<sub>1</sub> mice on day 0. Drugs administered iv on day 1 or ip on days 1, 5, and 9, following tumor implantation. <sup>b</sup> Primary colon C26 carcinoma (tripan blue excluding,  $2.5 \times 10^5$  cells/mouse) implanted in CDF<sub>1</sub> mice on day 0; drug administered ip on days 1, 5, and 9. <sup>c</sup> OD, optimal dose in milligrams/milliliter of vehicle, and administered iv or ip in 0.1 mL of vehicle (5% v/v Me<sub>2</sub>SO-saline). <sup>d</sup> MST, median survival time in days of tumor bearing and non-drug-treated (control) or drug-treated mice. <sup>e</sup> %ILS, percent increase in life span of drug-treated groups over the control group of test animals, excluding survivors. <sup>f</sup> (surv), number of sixty day survivors/number of mice treated with drug.

ID<sub>50</sub> values) by these enantiomers do not appear to be directly related to their gross proficiency for DNA or RNA inhibition. Evidently, factors other than only the inhibition of gross DNA and RNA synthesis parameters might be more significant for their tumor cell growth inhibitory activity; this action may depend more closely on other subtle effects, namely irreversible inhibition of specific nucleic acid sequences due to site-selective alkylation of dG bases in DNA, which could be more lethal than the binding at less sensitive sites; the specificity for binding to DNA sequences by the enantiomers is being investigated by standardized procedures.<sup>10,23</sup>

**Biological Activity in Vivo.** It has been reported in a previous paper<sup>1</sup> that the analogue (±)-EPA at the optimal dose level demonstrates 2.5 times the percent increase in median life time (%ILS) of P388/S lymphocytic leukemia in CDF<sub>1</sub> mice over that effected by AMD. P388/S is highly responsive to the action of AMD. In order to examine a broader spectrum of activity, these optical isomers were tested in two other mouse leukemia cell lines in vivo. One cell line, P388/ADR, is a derivative of the above P388/S made resistant to intercalating agents like actinomycin D but not to alkylating agents like mitomycin C.<sup>18</sup> Against this ip implanted tumor in CDF<sub>1</sub> mice, on a schedule of treatment by drugs on days 1–9, the %ILS jumped 10-fold, from a value of 33 for actinomycin to a value of 344 for racemic EPA [(±)-3b], with four out of 10 animals treated surviving over 60 days. The R-(+) and S-(-) enantiomers showed %ILS values of 400 and 377 with two and three out of 10 animals surviving >60 days, respectively. This remarkable improvement of activity in all the optically active or racemic forms of this analogue is matched by another alkylating agent, mitomycin C, which is known to act in cells via alkylation of DNA. Presumably, the high activities of these agents are derived primarily from their DNA-alkylating property (Table III).

When these agents were tested against another standard leukemia line, L1210 in CDF<sub>1</sub> mice, inoculated ip with tumor and treated with ip regimen of drugs administered on days 1, 5, and 9 after tumor inoculation on day 0, the activities of the optical isomers showed measurable differences in terms of %ILS and in the number of long-term survivors (Table V). In this leukemia line, in which actinomycin D is only moderately active, all three enantiomers demonstrated high activity, superior to those of actinomycin D. As observed earlier, the R-(+) form is

clearly the most active form with respect to %ILS (199) and in producing more long-term survivors (three out of nine), than either the racemic or the S-(-) enantiomer (Table V). In addition, the optimum dose levels of all the isomers are equivalent and are about double that of actinomycin, although the potencies of these agents in vitro are found superior to actinomycin. This might reflect an altered tumor vs host toxicity relationship (Table V) for these agents and suggest a subtle difference in the pharmacodynamic behavior of the active species in the tumor and the host. This is an important parameter that should be examined in order to elucidate the mechanism of action of these enantiomers both in tumors in vivo and in host organs.

The enantiomers also demonstrated superior activity to those of AMD in the treatment of two solid tumors in mice, e.g., B16 melanoma and C26 colon carcinoma (Table VI). Subcutaneously implanted B16 melanoma in BDF<sub>1</sub> mice is a slow growing tumor, but its rate of growth becomes faster when it is implanted ip. Against the ip implanted tumor, ip administered actinomycin is only moderately active; however, against sc implanted tumor, iv administered actinomycin is only marginally active. Compared to AMD, (±)-EPA and its enantiomer show improved activity in both ip and sc implanted tumor in respect of %ILS as well as number of long-term survivors, with the R-(+) enantiomer demonstrating the highest activity (Table VI). In an apparent anomaly, (±)-EPA demonstrates an equiactivity to that of the R-(+) isomer, which is higher than that shown by the S-(-) enantiomer in the ip vs ip treatment (Table VI). This is not consistent with data in other tumors; however, in this connection it should be pointed out that the combined effects of drugs (or enantiomers in this case) can be manifested in several ways, i.e., they can be synergistic, additive, or subtractive.

The C26 colon carcinoma implanted ip in CDF<sub>1</sub> mice (Table VI) also respond more favorably to the treatment by EPA enantiomers, with (R)-(+)-EPA, acting as the isomer of choice, demonstrating a higher %ILS and producing a larger number of long-term survivors. However, this superior activity in C26 tumor is less significant, in comparison to the clinically active agent adriamycin, which was used as a reference drug, and which is established as the drug of choice against solid tumors in general.

In brief, compared to the previously mentioned faster growing leukemias, the activities of EPA and enantiomers in the solid slower growing tumors are less pronounced. Nonetheless, all the optical isomers of EPA and particularly the R-(+) enantiomer show uniformly superior activity in comparison to the parent drug actinomycin D. AMD is known to be effective primarily against slow growing tumors in humans, e.g., Wilm's tumor in child-

(23) Hurley, L. H.; Leslie, F. In *Approaches Toward the Design of Sequence-Specific Drugs for DNA*, Annual Reports in Medicinal Chemistry; Bailey, D. M., Editor-in-chief; Academic: New York, 1987; Vol. 22, pp 259–268 and the references quoted therein.



ren,<sup>11</sup> choriocarcinoma in pregnant women, and Kaposi's sarcoma in AIDS disease patients.<sup>12</sup> The activities of this alkylating analogue EPA show promise for a superior activity against these tumor lines, with the additional prospect of a broader range of antitumor activity in faster growing leukemias and other tumors that are not responsive to actinomycin.

### Summary and Conclusions

The analogue of actinomycin D substituted with an epoxy function has recently been resolved into its optical antipodes of which the *R*-(+) enantiomer is superior in activity to the *S*-(-) enantiomer in several experimental murine tumors. Of these, the most promising activity is evident against ip implanted L1210 and P388/ADR leukemia, and B16 melanoma. The activity of this superior enantiomer is apparently derived from its DNA-alkylating activity and, more precisely, from site-specific alkylation of deoxyguanosine in the target molecule DNA. All these results make EPA and its enantiomeric forms promising candidate agents, worthy of investigation in a number of challenging tumor lines, for a comprehensive evaluation of their antitumor activity. Also, the compounds need to be tested in several animal species for evaluation of their toxicological, pharmacodynamic, and pharmacokinetic properties.

### Experimental Section

**Materials and Methods.** Chloropyruvic acid was prepared by the method of Cragoe and Robb<sup>13</sup> and was converted to methyl esters of *L*- $\beta$ -chloro- and *D*- $\beta$ -chlorolactic acids by the method of Herschbein and Whitesides.<sup>14</sup> DL- $\beta$ -Chlorolactic acid was purchased from ICN Pharmaceuticals. *L*- $\beta$ -Bromolactic acid was prepared via the reported procedures<sup>15</sup> from DL-3-bromopropane-1,2-diol, which was purchased from Aldrich. (*R*)-(+)- $\alpha$ -Methoxy- $\alpha$ -(trifluoromethyl)phenylacetic acid was purchased from Aldrich and was converted to its acid chloride by the method of Dale and Mosher.<sup>16</sup> Actinomycin D, NSC 3035 (lot L 55461-0) was purchased from Calbiochem, and [<sup>3</sup>H]actinomycin D was purchased from Amersham. The nucleosides were obtained from Collaborative Research and radiolabeled nucleotides from New England Nuclear. All samples were checked for purity by HPLC before use. Calf thymus DNA, protein-free, type 1 from Sigma was further purified by phenol extraction. All organic solvents were AR grade. THF was distilled from calcium hydride, and methanol was distilled from magnesium. All other solvents were freshly distilled before use. Water was deionized and distilled with a Corning Model 3B still. Argon and nitrogen were purified grade. Volumetric transfers were accomplished by using Hamilton syringes, and the reagents were added to reaction mixtures by using a variable-speed LKB 2120 peristaltic pump. All reactions were done in subdued light with a siliconized glass apparatus. Sephacryl S-200 and dextrans were purchased from Pharmacia Fine Chemicals and alkylamine-functionalized porous beads (CRG550) from Pierce Chemical Co. Pirkle I-A Chiralpak HPLC columns (Regis Chemical Co.) and MC-10 C<sub>18</sub> columns (Varian Instrument Co.) were primarily used in HPLC separations. Thin-layer chromatographic silica gel plates were from E. Merck Laboratories and Brinkman Instrument Co., and alumina plates were from Eastman Kodak. Solvent systems were (A) EtOAc-acetone (4:1), (B) 1-butanol-H<sub>2</sub>O-EtOH (4:1:1), and (C) Ciferi, the organic phase of the mixture EtOAc-MeOH-H<sub>2</sub>O (20:1:20). Poly(acrylamide-co-*N*-(acryloxy)succinimide) substrates (PAN) used for the attachment of enzymes were prepared as reported.<sup>17</sup> *L*-Lactic dehydrogenase (EC 1.1.1.27), *D*-lactic dehydrogenase (EC 1.1.1.28), glucose 6-phosphate dehydrogenase (EC 1.1.1.49),  $\beta$ -NAD<sup>+</sup>, and  $\beta$ -NADH were purchased from Sigma. Mitomycin C was purchased from Sigma, and Adriamycin was obtained as a gift from the Dana-Farber Cancer Center, Boston. All elemental analyses were within  $\pm 4\%$ . High-performance liquid chromatography was performed on a Varian Model 5020 gradient liquid chromatograph equipped with a CD-111L chromatography data system and with UV-visible variable- and fixed-wavelength detectors; columns were fitted with a Supleco guard column. Spectra

were determined on the following instruments: IR spectra were taken on a Perkin-Elmer Model 457A spectrometer in KBr micro pellets or chloroform solutions; UV-visible spectra were measured on a Gilford 250 spectrophotometer with use of 1- and 10-cm path length cells; this instrument was also used with the addition of a base-line reference compensator (Analog Multiplexer 6064), thermoprogammer, and auto four cell programmer and a thermoelectric cell holder for thermal denaturation studies of DNA-drug complexes ( $\Delta T_m$  value determinations). Specific rotations were measured in a JASCO-5UV/ORD spectropolarimeter. NMR spectra were obtained on a JEOL 90-90MHZ or 300-MHZ Varian XL-300 spectrometer. Specific activity were determined in a Packard Tricarb Model 1500 spectrometer.

DNA-binding experiments were carried out in 0.01 M phosphate buffer (pH 7), containing EDTA ( $10^{-5}$  M). For unwinding studies with covalently closed circular DNA, SV40 DNA (0.235  $\mu$ g, BRL, Bethesda, MD) was dissolved in 10 mM Trizma base (pH 7.4) buffer containing 50 mM KCl, 50 mM MgCl<sub>2</sub>, and 0.1 mM EDTA and incubated with appropriate volumes of drug solution for 60 min at 37 °C. After the addition of loading buffer (25% bromophenol blue, 25% xylene cyanol in 30% glycerol), each sample was added to a 1% agarose gel. The gels were run at 35 V overnight using a Tris-borate EDTA buffer (pH 8). The DNA was visualized by staining the gel with ethidium bromide (0.5  $\mu$ g/mL).

**UV Identification of the Deoxyguanosine Adducts.** ( $\pm$ )-EPA and enantiomers, 1.7 mM (1 mL) were incubated with deoxyguanosine (17 mM, 1 mL) in 0.5 Tris-HCl buffer (pH 7.4) at 37 °C for 16 h according to the method reported recently.<sup>21</sup> At the end of incubation, the samples were extracted thoroughly with methylene chloride to remove any unreacted ( $\pm$ )-EPA, ( $\pm$ )-DHPA, or enantiomers. The reaction products were first chromatographed on a Sephadex LH-20 column and eluted, according to our procedure,<sup>2</sup> with 20% MeOH-H<sub>2</sub>O (v/v) and 50–80% MeOH-H<sub>2</sub>O in a linear gradient. After evaporation of the eluates, the residue was separated on a HPLC (Varian 5020) equipped with a C-18, 7.5  $\times$  250 mm column, particle size 5  $\mu$ m. A gradient of water-methanol 65–90% at a concave gradient and at a flow rate of 1 mL/min for 150 min was used. Four EPA-dG adducts were isolated corresponding to peaks at retention times 45 min (EPA I-dG), 75 min (EPA II-dG), 85 min (EPA III-dG) and 110 min (EPA IV-dG) (Figure 3).

These deoxyguanosine adducts exhibit characteristic substitution-dependent UV spectra in neutral, alkaline, and acid solutions (20 °C, pH 1–13); the required pHs of these solutions were adjusted by mixing 50 mM sodium phosphate buffer with NaOH and HCl. Sites of substitution on deoxyguanosine were indicated from the UV peaks, which were found in close agreement with those reported for authentic guanosine adducts<sup>21</sup> (Table IV). Furthermore, one of the adducts, N<sup>7</sup>-substituted guanosine, which was found unstable in acid pH (0.1 N HCl) was incubated for 30 min at 70 °C, neutralized to pH 8.0, and extracted to EtOAc. The residue, on evaporation, was subjected to HPLC after increasing the gradient to 90% methanol at 2 mL/min. Two peaks, one minor, 120 min (~20%), and the other major, 135 min (75%), were isolated. N<sup>7</sup>-Deoxyguanosine EPA IV-dG elutes at 95 min in this system. The major peak material from the model analogue was subjected to mass spectrometric analysis: MS, *m/z* 589 (M – H).

**Methyl  $\beta$ -Chlorolactates.** The methyl esters of DL-, *D*-, and *L*- $\beta$ -chlorolactic acid were prepared according to the procedure reported by Hirschbein and Whitesides:<sup>14</sup> <sup>1</sup>H NMR (CDCl<sub>3</sub>)  $\delta$  4.53 (t, 1 H, methine), 3.60 (s, 3 H, methyl), 3.40 (d, 2 H, methylene), 4.90–5.5 (variable, OH, exchangeable with D<sub>2</sub>O); IR (neat) 3530 (OH), 2990 (C–H), 1745 cm<sup>-1</sup> (carbonyl); [ $\alpha$ ]<sub>D</sub><sup>20</sup> +4.4  $\pm$  0.09° for *D*-, -4.08  $\pm$  0.09° for *L*-, and 0° for DL- (c CHCl<sub>3</sub>, 1.0 g/100 mL). Anal. (C<sub>4</sub>H<sub>7</sub>ClO<sub>3</sub>) C, H, N, Cl.

**Methyl  $\beta$ -bromolactates** were prepared as above from DL- or *L*- $\beta$ -bromolactic acid: <sup>1</sup>H NMR (CDCl<sub>3</sub>)  $\delta$  4.55 (m, 1 H), 3.60 (s, 3 H), 3.50 (d, 2 H), 5.50 (br, OH). Anal. (C<sub>4</sub>H<sub>7</sub>BrO<sub>3</sub>) C, H, N.

***N,N*-Dimethyl-3-(benzyloxy)-2-nitro-*p*-toluenecarboxamide.** This compound was prepared via our reported procedure<sup>3</sup> with the corresponding acid chloride and diethylamine in the ratio of 1:5 mol; the product crystallized from 5:1 ether-petroleum ether (bp 30–60 °C) yielded 75% white solid: mp 63–65 °C;  $\lambda_{\max}$  (EtOH)

( $\epsilon$ ) 224 (26 000), 289 nm (1560). Anal. ( $C_{17}H_{18}N_2O_4$ ) C, H, N. **2-Amino-1,9-bis(*N,N*-dimethylcarbamoyl)-4,6-dimethyl-3*H*-phenoxazin-3-one (1a).** The above 3-(benzyloxy)-2-nitrotoluic acid derivative was reductively debenzylated, and the intermediate aminophenol was self-condensed with a second unit with use of  $K_3Fe(CN)_6$  to produce red crystals: mp 188–189 °C (95%);  $\lambda_{max}$  (EtOH) ( $\epsilon$ ) 226 (926 000), 432 nm (18 000);  $^1H$  NMR  $\delta$  7.20, 7.38 (dd, 2 H, Ar H), 2.55 (s, 3 H,  $CH_3$ ), 2.35 (s, 3 H,  $CH_3$ ), 5.01 (s, 12 H,  $NCH_3$ ), 5.55 (s, 2 H,  $NH_2$ ) in  $CDCl_3$ . Anal. ( $C_{20}H_{22}N_4O_4$ ) C, H, N.

**2-Amino-1,9-bis(*N,N*-dimethylcarbamoyl)-4,6-dimethyl-7-hydroxy-3*H*-phenoxazin-3-one (2a).** Via our previously reported procedure<sup>3</sup> for the 7-hydroxy analogues and with compound 1a as the starting material, 2a was obtained in 76% overall yield: mp 265–258 °C;  $\lambda_{max}$  ( $CHCl_3$ ) ( $\epsilon$ ) 458 nm (19 000);  $^1H$  NMR  $\delta$  6.78 (s, 1 H, Ar H), 2.0 and 2.22 (s, 6 H,  $CH_3$ ), 5.21 (s, 12 H,  $NCH_3$ ) in  $CDCl_3$ . Anal. ( $C_{20}H_{22}N_4O_5$ ) C, H, N.

**7-[2-Hydroxy-2-(methoxycarbonyl)ethoxy]actinomycin D [( $\pm$ )-4b] and *R*-(-) and *S*-(+)-Enantiomers [( $\pm$ )-4b and (+)-4b].** These optical isomers were made with 7-hydroxyactinomycin D (2b) as starting material and coupling with ( $\pm$ ), (-), or (+) isomers of  $\beta$ -chloro- or  $\beta$ -bromolactic acid methyl esters via previously reported procedures<sup>4</sup> at 45–60 °C. When  $\beta$ -chloroacetic acid was employed, a longer (28–38 h) reaction time was necessary compared with the 16–20-h reaction time for  $\beta$ -bromolactates. Yields of reaction with bromo esters were always better (55–66%) than with the chloro esters (35–50%). Reaction in a dry argon atmosphere helped to prevent decomposition of products: IR (KBr) 35510 (secondary OH), 3520 (primary OH), 1745  $cm^{-1}$  (carbonyl);  $\lambda_{max}$  ( $CHCl_3$ ) 460 nm ( $\epsilon$  18 700); mp 200–205 °C (Table II for properties). Anal. ( $C_{66}H_{92}N_{12}O_{20} \cdot 2H_2O$ ) C, H, N.

**Compound 4a:** mp 200–208 °C;  $\lambda_{max}$  ( $CHCl_3$ ) 458 nm ( $\epsilon$  20 000) (Table I for physical properties). Anal. ( $C_{24}H_{28}N_4O_8$ ) C, H, N.

**Racemic ( $\pm$ )-7-(2,3-Dihydroxypropoxy)actinomycin D [( $\pm$ )-5b], and Its *R*-(-) and *S*-(+)-Enantiomers.** Compound 4b and its enantiomers (0.02 mol) in dry tetrahydrofuran (THF) solution were treated with 0.1 M  $LiBH_4$  in pyridine (1 mL). After the mixture was stirred for 1 h in argon, the excess reducing agent was quenched with dropwise addition of cold (0 °C) water, and the mixture was centrifuged. The solvent was separated from the precipitated lithium by aspiration, the precipitate was centrifuged twice with THF (5 mL), and the combined THF fractions were evaporated. The product showed complete conversion of the ester to the corresponding hydroxy analogue as evidenced by the absence of the IR 1745  $cm^{-1}$  peak of the ester carbonyl; the quinone and amide carbonyl peaks appear at 1710 and 1700–1720  $cm^{-1}$ ; yield 30–45%, mp 286 °C dec for ( $\pm$ )-5b, and compound ( $\pm$ )-5a prepared similarly, mp 200 °C, was identical with previously reported,<sup>1</sup> yield 33% (Tables I and II for properties).

**Racemic ( $\pm$ )-7-[2-Hydroxy-3-(tosyloxy)propoxy]actinomycin D [( $\pm$ )-6b] and *R*-(-) and *S*-(+)-Enantiomers.** Compound 5b (0.15 mmol) and enantiomers were allowed to react in 0.15 M solution in pyridine with *p*-toluenesulfonyl chloride (0.135 mmol, 0.135 M in pyridine) for 30 h at 0 °C in an argon atmosphere. The reaction mixture was extracted with 5 volumes of ether and washed successively with 1 N HCl and water to remove pyridine. The residue after evaporation was purified on a silica gel TLC (E. M. Laboratories, EtOAc–acetone, 3:1). Unreacted dihydroxy starting compound,  $R_f$  0.28–0.30, separated (50%) from the tosyloxy derivative 6b,  $R_f$  0.47–0.53. The pure *R*-(-) and *S*-(+)-derivatives were separated by HPLC, yields 50% and 43%, respectively: mp 192 °C;  $\lambda_{max}$  ( $CHCl_3$ ) ( $\epsilon$ ) 262 (19 000), 465 nm (11 000); IR (KBr) 3510 (OH), 1590, 1480, 1330 ( $\nu_{as}$ ,  $SO_2$ ), 1170 ( $\nu_s$ ,  $SO_2$ ). (Tables I and II for other physical properties). Anal. ( $C_{72}H_{98}N_{12}O_{21}S$ ) C, H, N, S.

**Compound 6a:** mp 109–110 °C;  $\lambda_{max}$  ( $CHCl_3$ ) 265 nm ( $\epsilon$  20 000), 465 ( $\epsilon$  10 000); yield 45–55%; TLC  $R_f$  0.56; IR peaks for OH and  $SO_2$  are same as in 6b (Tables I and II for data). Anal. ( $C_{30}H_{34}N_4O_9S$ ) C, H, N, S.

**Racemic ( $\pm$ ), *R*-(+), and *S*-(-) Enantiomers of 7-(2,3-Epoxypropoxy)actinomycin D (3b).** Tosyloxy derivatives of the racemic, *S*-(+), and *R*-(-) optical forms (6b, 0.1 mmol) in 50 mL of 1.5% (w/v) methanolic KOH were stirred at ambient temperature (21 °C) for 3 h. The reaction was monitored by TLC

on Alumina plates (Eastman, *n*-butanol–water–ethanol, 4:1:1) for P-lactonic ring opened products.<sup>5</sup> Simultaneously the conversion of the oxirane ring to the desired products was indicated by the appearance of spots at  $R_f$  0.35 of 3b only (E. M. Laboratories silica gel plates, EtOAc–acetone, 4:1) and disappearance of 6b. The reaction was diluted with 4 volumes of  $CH_2Cl_2$  and washed with water to remove KOH (to pH 7.8). After drying ( $Na_2SO_4$ ) and evaporation, the residue was crystallized from (*n*-hexane–ether, 1:1): mp 212 °C; yield 66% for *R*-(+), 40% for *S*-(-), and 53% for the racemic ( $\pm$ ) forms; racemic material was identical with previously reported material.<sup>1</sup> Anal. ( $C_{62}H_{90}N_{12}O_{18} \cdot 2H_2O$ ) C, H, N.

**Compound 3a enantiomers:** mp 222–225 °C; yields 35–55%. Anal. ( $C_{23}H_{26}N_4O_6$ ) (Tables I and II for properties).

**Bis[(*R*)-(+)- $\alpha$ -methoxy- $\alpha$ -(trifluoromethyl)phenylacetyl] [(*R*)-(+)-MTPA] Ester Derivatives of 7-(2,3-Dihydroxypropoxy)actinomycin D (7b).** Samples of 5b (0.15 mmol) in  $CCl_4$  (5 mL) with distilled MPTA chloride in 0.5 mL pyridine at 20 °C were stirred for 20 h in  $N_2$ . Water (2 mL) was added, and the mixture was transferred to a separatory funnel with  $CHCl_3$ . The organic phase was washed sequentially with dilute HCl,  $NaHCO_3$ ,  $H_2O$  and dried (anhydrous  $Na_2SO_4$ ). The residue was purified on preparative silica gel TLC plates (EtOAc–acetone, 4:1). The major band,  $R_f$  0.59–0.63, was extracted with  $CHCl_3$  and crystallized from a 1:1 mixture of THF–pentane, and the pure materials were identified by  $^{19}F$  NMR and HPLC (data in Table II): mp 282 °C dec; yield for *R*-(+), *S*-(+), 65%; *R*-(+), *R*-(-), 69%. Anal. ( $C_{85}H_{106}N_{12}O_{23}F_6$ ) C, H, N.

**Compound 7a:** mp 219–223 °C;  $R_f$  0.66; yield 80% (Table I for data). Anal. ( $C_{43}H_{42}N_4O_{11}F_6$ ) C, H, N.

**Binding to DNA. Intercalative and Covalent Binding to DNA. Isolation and Identification of DNA–EPA Enantiomer Adducts.** These experiments were performed with either (*R*)-(+)-EPA or (*S*-(-)-EPA and calf-thymus DNA according to our previously reported procedures.<sup>2</sup>

**Acknowledgment.** This work was supported by a grant (NCI, CA-26281) from the National Institutes of Health. We gratefully acknowledge J. Anderson for the synthesis of the early compounds and Christine Kelley, Mary Anne Guire, and Josephine Szabo in conducting the evaluation of *in vivo* and *in vitro* tests. We are also grateful to Albert Ross and Jacob J. Clement of Arthur D. Little Co., Cambridge, MA, for supplying many tumor lines in mice.

**Registry No.** 1a, 114635-23-3; 1b, 50-76-0; 2a, 114635-24-4; 2b, 21478-73-9; ( $\pm$ )-3a, 114635-30-2; (*R*)-3a, 114715-28-5; (*S*)-3a, 114715-29-6; 3b, 82830-18-0; (*R*)-3b, 114715-30-9; (*S*)-3b, 114715-31-0; ( $\pm$ )-4a, 114635-27-7; (*R*)-4a, 114715-20-7; (*S*)-4a, 114715-21-8; 4b, 114635-26-6; (*R*)-4b, 114715-18-3; (*S*)-4b, 114715-19-4; ( $\pm$ )-5a, 114635-28-8; (*R*)-5a, 114715-24-1; (*S*)-5a, 114715-25-2; 5b, 82830-19-1; (*R*)-5b, 114715-22-9; (*S*)-5b, 114715-23-0; ( $\pm$ )-6a, 114635-29-9; (*R*)-6a, 114715-26-3; (*S*)-6a, 114715-27-4; 6b, 114651-85-3; (*R*)-6b, 114716-22-2; (*S*)-6b, 114716-23-3; (*S*)-7a, 114635-32-4; (*R*)-7a, 114715-33-2; (*S*)-7b, 114635-31-3; (*R*)-7b, 114715-32-1; (*S*)-(+)-MTPA chloride, 20445-33-4; *N,N*-dimethyl-3-(benzyloxy)-4-methyl-2-nitrobenzenecarboxamide, 114635-22-2; DL- $\beta$ -chlorolactic acid, 50906-02-0; D- $\beta$ -chlorolactic acid, 82079-44-5; L- $\beta$ -chlorolactic acid, 61505-41-7; DL-methyl  $\beta$ -bromolactate, 114635-25-5; L-methyl  $\beta$ -bromolactate, 114715-17-2; (*R*)-EPA- $N^7$ -guanosine conjugate (isomer 1), 114635-33-5; (*R*)-EPA- $N^7$ -guanosine conjugate (isomer 2), 114635-34-6; (*R*)-EPA- $O^6$ -guanosine conjugate (isomer 1), 114635-35-7; (*R*)-EPA- $O^6$ -guanosine conjugate (isomer 2), 114635-36-8; deoxyguanosine, 961-07-9.

**Supplementary Material Available:** Figure 1 demonstrating the agarose (1%) gel electrophoresis of ccc-SV40 DNA intercalated with enantiomeric analogues of actinomycin D, actinomycin D and EBr, Figure 2 depicting relative circular dichroism of the enantiomers of ( $\pm$ )-EPA-dG adducts, and Figure 3 illustrating the probable stereochemistry and conformation of the deoxyguanosine adducts derived from the *R*-(+) and *S*-(-) forms of EPA, respectively (3 pages). Ordering information is given on any current masthead page.